

Monopole and vortex content of a meron pair

Álvaro Montero⁽¹⁾ and John W. Negele⁽²⁾

(1) Department de Física Fonamental
Universitat de Barcelona
Barcelona 08028
Spain
e-mail: montero@ffn.ub.es

(2) Center for Theoretical Physics
Laboratory for Nuclear Science and Department of Physics
Massachusetts Institute of Technology
Cambridge, Massachusetts 02139
USA
e-mail: negele@mitlns.mit.edu

ABSTRACT

We investigate the monopole and vortex content of a meron pair by calculating the points at which the transformation to the Laplacian Center Gauge is ill-defined and by studying the behavior of Wilson loops. These techniques reveal complementary aspects of the vortex and monopole structure, including the presence of closed monopole lines and closed vortex surfaces joining the two merons, and evidence for intersecting vortex surfaces at each meron.

PACS: 11.15.-q; 12.38.Aw

Keywords: Yang-Mills theory; Monopoles; Center vortices; Laplacian Center gauge.

1 Introduction

The QCD vacuum is characterized by two striking phenomena, the breaking of chiral symmetry and the confinement of color charge. Chiral symmetry breaking may be understood in terms of localized topological excitations of the gluon field and their associated quark zero-modes that produce a non-vanishing value of the chiral condensate. Classical instanton [1] solutions of the Yang Mills equations with topological charge $Q = 1$ and their quantum fluctuations provide a physical foundation for these topological excitations and thus a natural understanding of chiral symmetry breaking.

In contrast, the mechanism for confinement is not presently well understood, and various pictures have been investigated to try to explain it in terms of relevant structures in the QCD vacuum. Various point-like solutions to the Yang Mills equations, which fall off at large distances in all space-time dimensions, have been considered. Although $Q=1$ instanton solutions provide an understanding of chiral symmetry breaking, in the dilute gas and instanton liquid approximations they do not lead to confinement [2]. Merons, topological charge $\frac{1}{2}$ solutions found by De Alfaro, Fubini and Furlan [3], are more strongly disordering objects than instantons and were proposed as a mechanism for confinement by Callan, Dashen and Gross [4]. Fractons, also solutions of the Yang Mills equations of motion with fractional topological charge, appear on the four-dimensional torus, T^4 , when twisted boundary conditions are imposed [5]. The possible relevance of these objects to confinement was pointed out in [6], and a scenario for confinement based on the fractional charge solution found in reference [7], was proposed by González-Arroyo and Martínez [8].

One and two-dimensional structures in the QCD vacuum have also been considered as mechanisms for confinement. In the dual superconductor picture [9], the condensation of monopoles in the QCD vacuum leads to confinement. Monopoles are one-dimensional curves in space-time that appear in QCD as defects in the abelian gauges proposed by 't Hooft [10]. The gauge is fixed up to the Cartan subgroup of the gauge group and monopoles appear at points in space where this gauge fixing is ill-defined, leaving a gauge freedom larger than the abelian subgroup. In the vortex theory [11], confinement is due to the condensation of vortices. Vortices are two-dimensional surfaces carrying flux in the center of the $SU(N)$ group, which means that a Wilson loop intersecting the surface of the vortex

takes the value of one of the elements of the center of the group. Classical vortex solutions to the $SU(N)$ Yang Mills equations have been found numerically [12].

The mechanism for chiral symmetry breaking and the alternative descriptions of confinement are not mutually exclusive - rather they are highly interrelated. The fact that the intersection of two vortices has topological charge $\frac{1}{2}$ [13–15] provides a provocative connection between chiral symmetry breaking and confinement and suggests that the confinement properties of charge $\frac{1}{2}$ merons may also be understood in terms of the intersections of vortices. In addition, as elaborated below, monopole lines lie on vortex surfaces, so that both structures coexist and may be studied simultaneously. In this picture, a meron pair corresponds to the intersection of two closed vortex sheets containing closed monopole loops and provides the simplest system in which one could explore this structure quantitatively. As the separation between the merons decreases to zero and they merge into an instanton, one would expect a vortex sheet and a monopole loop on it to shrink to a point at the center of the instanton [16,17]. A similar picture of the separation of an instanton into two fractionally charged objects connected by hedgehog world lines is given in reference [18].

In this article we investigate numerically the monopole and vortex content of a meron pair in $SU(2)$ Yang Mills theory by calculating the points at which Laplacian Center Gauge fixing is ill-defined [19,20] and by calculating the behavior of Wilson loops. The monopole and vortex content of an isolated meron has already been studied analytically by Reinhardt and Tok [21] using Laplacian Center Gauge fixing and Wilson loops, and provides an essential foundation for the present work. Since their work, as well as that of others, has shown Laplacian Center Gauge fixing to be an imperfect tool, in this study we also explore the limitations of this tool as well as the physics of the QCD vacuum.

The outline of this letter is the following. In section 2 we describe the meron pairs that we study and in section 3 we use Wilson loops to explore their vortex content. Section 4 presents the monopole and vortex content of these configurations determined from Laplacian Center Gauge defects and section 5 summarizes our conclusions.

2 The meron pair

Merons [3] are solutions to the classical Yang-Mills equations of motion in four Euclidean dimensions, which can be written as

$$A_\mu^a(x) = \eta_{a\mu\nu} \frac{x^\nu}{x^2} , \quad (1)$$

where $\eta_{a\mu\nu}$ is the 't Hooft symbol. Using the conformal symmetry of the classical Yang-Mills action, it can be shown that in addition to a meron at the origin, there is a second meron at infinity, and these two merons may be mapped to arbitrary positions. The gauge field for the two merons [3] is

$$A_\mu^a(x) = \eta_{a\mu\nu} \left[\frac{x^\nu}{x^2} + \frac{(x-d)^\nu}{(x-d)^2} \right] . \quad (2)$$

This gauge field for the meron pair has infinite action density at points $x_\mu = \{0, d_\mu\}$. To avoid the problem of these singularities, we use the following expression [4]

$$A_\mu^a(x) = \eta_{a\mu\nu} x^\nu \begin{cases} \frac{2}{x^2 + r^2} , & \sqrt{x^2} < r , \\ \frac{1}{x^2} , & r < \sqrt{x^2} < R , \\ \frac{2}{x^2 + R^2} , & R < \sqrt{x^2} . \end{cases} \quad (3)$$

Here, the singular meron fields for $\sqrt{x^2} < r$ and $\sqrt{x^2} > R$ are replaced by instanton caps, each containing topological charge $\frac{1}{2}$ to agree with the topological charge carried by each meron. We study the monopole and vortex content of this configuration by putting the gauge field on a lattice of size $N_t \times N_s^3$. For details of the procedure for putting the meron pair on the lattice and relaxing it to a solution of the field equations, see reference [22].

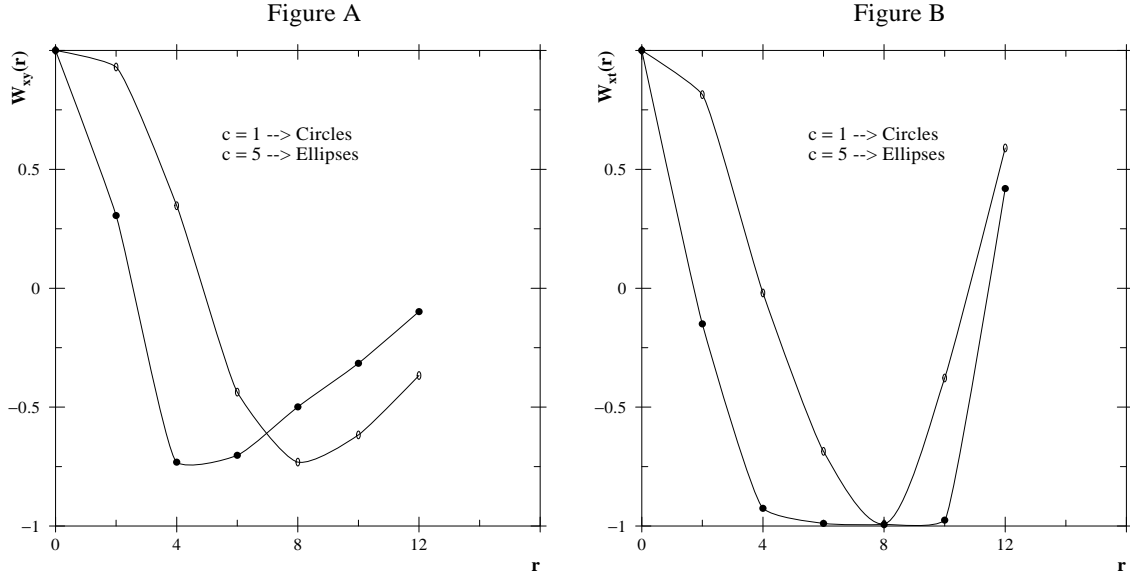
In this article, we analyze four meron pair configurations obtained on $N_t \times N_s^3$ lattices with $N_s = 16, 24$ and $N_t = 2N_s$. We study configurations with different cap sizes, c , distances between merons, d , and sizes of the lattice, N_s . We used a configuration with $N_s = 16$, $c = 4$ and $d = 10$ (configuration I), and three configurations with $N_s = 24$: one with $c = 1$ and $d = 12$ (configuration II), one with $c = 5$ and $d = 12$ (configuration III), and one with $c = 1$ and $d = 16$ (configuration IV). We have checked that the field strength from each

of the lattice configurations has the essential properties described in reference [22] for the continuum field strength. We have also applied up to five cooling sweeps to the meron pair configurations in order to relax them close to lattice solutions, and checked that the monopole and vortex content for these meron pair configurations are independent of this cooling. Although we do not explicitly address Dirac zero modes in this work, note that the zero mode for a meron pair configuration has been calculated for a range of separations in reference [22] and displays two peaks at the positions of the merons.

3 Vortex content from Wilson loops

Before considering Laplacian Center Gauge fixing, it is useful to describe the vortex content obtained from calculating Wilson loops. For a single, singular meron at the origin, it has been shown that a circular Wilson loop around the origin in any of the six planes defined by a pair of coordinate axes (x, y, z, t) has the value -1 for any size of the circle [21]. Hence, Wilson loops indicate the presence of a vortex surface on all the planes defined by pairs of coordinate axes. For our configurations, regularized meron pairs, we studied two sets of Wilson loops. For the xy , xz or yz plane, planes orthogonal to the line joining both merons, we calculated a square Wilson loop of size $r \times r$ with one of the merons in the center of the loop. The results for configurations II and III (distance between merons $d = 12$ and cap sizes $c = 1, 5$), and for the xy plane, are shown in figure 1A. We see that at short distance, the value of the Wilson loop goes from $+1$ towards the value -1 , as for a single meron, and only changes this behavior at large distance where the contribution of the second meron starts to be significant, approaching the value $+1$ when the loop is bigger than the distance between the merons. We also see in figure 1A the effect of the cap size. The cap gives a characteristic size c to the meron, which is reflected in the distance one must go for the value of the Wilson loop to start to be approach -1 and thus enclose the vortex flux. Note that for the original singular meron, this size would be zero. The results obtained for the other two planes, xz and yz , are the same, showing the underlying spherical symmetry in the spatial directions of the meron pair. Results for the other two configurations were completely analogous, with the curves simply reflecting the corresponding cap sizes and separation between merons.

Figure 1: Wilson loops for a meron pair. Figure A shows the values of $r \times r$ Wilson loops in the xy plane centered at the maximum of one of the merons as a function of r for configurations with separation $d=12$ and cap sizes $c = 1$ and 5 (configurations II and III). Figure B shows the values of $r \times 2r$ Wilson loops in the xt plane centered at the maximum of one of the merons as a function of r for the same configurations as in figure A. In both figures, lines are plotted joining the calculated points to guide the eye.



For the xt , yt or zt planes, which include the line joining both merons, we calculated a rectangular Wilson loop of size $r \times 2r$ with one of the merons in the center of the loop. The results in the xt plane for the same configurations as in figure 1A, are shown in figure 1B. We see that again at short distances, the Wilson loop goes from $+1$ to -1 as the size of the loop increases, and as r exceeds half the separation between merons, the Wilson loop begins to approach $+1$, which it will reach when both merons are included. Again, the loop must be larger than the cap size, c , to enclose all the vortex flux. As before, the results for the other two planes, yt and zt , are the same, and the other configurations show analogous behavior reflecting the other cap sizes and separations.

The conclusion from this study of Wilson loops in a meron pair is that, like an isolated meron, a meron in a pair behaves like a source or sink for flux in non-trivial elements of the center of the group for all six planes defined by the Cartesian axes, and the size of the source or sink is of order of the cap size, c . Thus, each meron corresponds to the

intersection of orthogonal pairs of vortices.

4 Monopole and vortex content from Laplacian Center Gauge defects

In this section, we present the monopole and vortex content of the meron pair configurations described in the previous section, as inferred from the points at which gauge fixing to the Laplacian Center Gauge is ill-defined.

Fixing the gauge to Laplacian Center Gauge [19, 20] involves the use of the two eigenvectors with lowest eigenvalues, $\psi_1^a(n)$ and $\psi_2^a(n)$, of the Laplacian operator,

$$\mathcal{L}_{nm}^{ab}(R) = \sum_{\mu} \left(2\delta_{nm}\delta^{ab} - R^{ab}(n, \mu)\delta_{m, n+\hat{\mu}} - R^{ba}(m, \mu)\delta_{n, m+\hat{\mu}} \right) \quad (4)$$

in the presence of a gauge field $R^{ab}(n, \mu)$ in the adjoint representation of the gauge group. The lowest eigenvector, $\psi_1^a(n)$, is rotated to the (σ_3) direction in color space. This step fixes the gauge up to the abelian subgroup of the $SU(2)$ group. The $U(1)$ abelian freedom is fixed by imposing the additional condition that the $\psi_2^a(n)$ eigenvector is rotated to lie in the positive (σ_1, σ_3) half-plane. After these two steps, the gauge is completely fixed up to the center degrees of freedom.

Monopoles and vortices are found in Laplacian Center Gauge as defects of the gauge fixing procedure, which means we have to look at the points at which the gauge fixing prescription is ill-defined. The first step, rotation of the first eigenvector to the third direction in color space, is ill-defined if $\psi_1^a(t, x, y, z) = 0$. This defines lines in four-dimensional space and these lines are identified as monopole lines. The second step, rotation of the second eigenvector to the positive (σ_1, σ_3) half-plane, is ill-defined at points at which the first and second eigenvectors are parallel. This condition defines surfaces in four dimensional space and these surfaces are identified as vortex sheets.

To fix to the Laplacian Center Gauge we use the algorithm presented in [23] to calculate the lowest eigenvectors of the Laplacian operator. We calculate the four eigenvectors with lowest eigenvalues, and find that the three lowest eigenvalues are degenerate. With two vectors chosen from these three, or from linear combinations of these three, we can fix

the gauge to Laplacian Center Gauge. Note that because of the degeneracy in the lowest eigenvalues, the monopole and vortex content is ambiguously defined, and in this work we will consider all the different monopole and vortex patterns that may be obtained from the lowest eigenvectors.

Before considering the monopole and vortex content of our meron pair configurations, it is useful to review the monopole and vortex content of two limiting cases, an instanton and a single meron. The eigenfunctions of the lowest state of the Laplacian for these two cases are known analytically [21]. For an isolated instanton there are three degenerate eigenfunctions, a monopole is only be located at the origin since it is the only point at which the eigenfunctions vanish, and there are no vortices because the three eigenfunctions are always mutually orthogonal. For the single meron, there are four degenerate eigenfunctions and the monopole content depends on the choice of lowest eigenvector. For the functions given in [21] it is easy to see that the i^{th} eigenvector has a monopole line along the i^{th} coordinate axis. We may think of this monopole line as joining the meron at the origin with the second meron at infinity, and the different lines arising from the different eigenvectors or combinations of them simply reflects the fact that the second meron may be reached at any position on the sphere at infinity. The vortex content also depends on the choice of the two lowest eigenvectors. It is easy to see that if one takes the i^{th} and j^{th} eigenvectors, the vortex content is given by the plane generated by the i^{th} and j^{th} coordinate axis. Taking other combinations of these four eigenvectors produces more complicated results, like one of the examples presented in [21], in which one obtains three vortex sheets given by three planes intersecting at the origin. It is noteworthy that this construction never generates the expected geometry of two intersecting vortices which in turn contain monopole lines, revealing that the Laplacian Center Gauge defects do not provide a completely satisfactory picture even in this analytically solvable case.

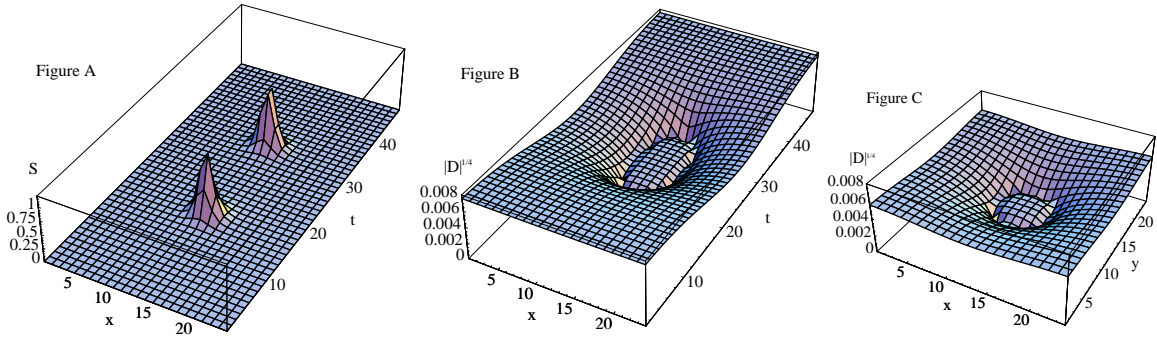
We now consider the monopole and vortex content of our meron pair configurations extracted from the three degenerate eigenvectors of the Laplacian. We will show that there is a vortex surface that looks like an ellipsoid of revolution touching the center of each meron at each tip, and that the monopole loops lie on this surface. The zeros in figures 2B and 2C correspond to longitudinal and axial sections of this surface respectively. The first quantity we examine is the modulus $\Psi(n) = \sqrt{\sum_{a=1}^3 (\psi^a(n))^2}$ and we look for points at

which $\Psi(n) = 0$. One of the problems we have to face is the different monopole pictures obtained by choosing different eigenvectors or a linear combinations thereof. We have looked for a combination in which the monopole content is particularly clear and found that it was useful to minimize the sum of the modulus in a specified plane by taking linear combinations of the three eigenvectors. Doing this, we have found a combination in which the first eigenvector, I, has a monopole loop in the xt plane joining the two merons, the second eigenvector, II, has the same monopole loop but in the yt plane and the third eigenvector, III, has the same monopole loop in the zt plane. A picture of the loop coming from eigenvector I, the loop in the xt plane, can be seen in figure 2B, which is explained in more detail below. The vortex content obtained from eigenvectors I, II and III is also quite clear. If we choose eigenvectors I and II as the two lowest eigenvectors, the vortex surface looks like an ellipsoid of revolution around the t axis in the xyt coordinates, with this surface including the monopole loop in the xt plane coming from eigenvector I and the monopole loop in the yt plane coming from eigenvector II. If we choose eigenvectors I and III as the two lowest eigenvectors, the vortex surface is the same but in this case in the xzt coordinates and if we choose eigenvectors II and III we see the same surface in the yzt coordinates.

To obtain the locus of all the points which can be monopoles or vortices for our meron configurations, we calculate the determinant of these three vectors, I, II and III, at each lattice point. First, note that if any of the vectors is zero, the condition to find monopoles, the determinant is zero. Second, note that if there is a linear combination between them giving a zero vector, the condition to find vortices, the determinant is also zero. Finally, note that the determinant is independent under linear combinations of the three vectors. Hence, all the points for our meron configurations that can be monopoles or vortices are determined by the condition that the determinant vanishes.

The result we obtain is the following. We find a region on the lattice in which the determinant is always positive and another one in which it is always negative, both regions separated by a three-dimensional volume in which the determinant vanishes and defines all positions that can be monopoles or vortices. We describe the shape of this volume by showing some of its two-dimensional sections. First, we show its temporal dependence. Consider the determinant as a function of x and t , for values of y and z fixed to the values

Figure 2: Figure A shows the action density $S(t,x,y,z)$ for the meron pair with $d = 16$ and $c = 1$ (configuration IV) as a function of x and t , with y and z fixed to the values that maximize the action density. Figure B shows the absolute value of the discriminant of the three lowest Laplacian eigenvectors, $D(t,x,y,z)$, to the $1/4$ power as a function of x and t , for the same meron pair configuration and values of the y and z coordinates used in figure A. Figure C shows the absolute value of $D(t,x,y,z)$ to the $1/4$ power as a function of x and y for z fixed to the value that maximizes the action density and t fixed to the midpoint between the two merons.



that maximize the action density for these coordinates. Figure 2B shows the absolute value of the determinant (raised to the $1/4$ power to see the curve more clearly). The curve on which the determinant vanishes is similar to an ellipse, and joins the two maxima of the action density in the x, t coordinates. To see that this loop joins the maxima in the action density to within a fraction of a lattice spacing, we show in figure 2A the action density as a function of x and t , and for the same fixed values of y and z . This loop is the same as the monopole loop described above defined by the points at which the modulus of eigenvector I vanishes. If we look at the determinant as a function of y and t (or z and t), and for values of x and z (or x and y) fixed to the maxima in the action density for these coordinates, we again obtain the same curves shown in figures 2A and 2B with x interchanged with y (or z). This curve in the y and t coordinates is also the monopole loop defined by the points at which the modulus of eigenvector II vanishes (and the curve in the z and t coordinates is the monopole loop defined by eigenvector III).

Second, we show the spatial dependence for fixed time positions. If we label the temporal positions for the maxima in the action density for each meron as t_1 and t_2 , we find that

for values of the lattice position t belonging to $[0, t_1]$ and $[t_2, N_t]$, the determinant is always positive for all points in the three-dimensional lattice defined at each temporal point. For values of t between the two merons, $t_1 < t < t_2$, we find a spherical surface in which the determinant changes sign, and inside the sphere the determinant is negative. The radius of this sphere at each temporal point may be seen in figure 2B, where it corresponds to half the width of the monopole loop at each temporal point. A section of this sphere is plotted in figure 2C, which shows the absolute value of the determinant $D(t, x, y, z)$ to the $1/4$ power as a function of x and y , with z fixed to the value that maximizes the action density and t fixed midway between the two merons. As claimed, this section is clearly observed to be circular.

We have obtained analogous results for all four configurations we have studied. The locus of all the points that can be monopoles or vortices is a three-dimensional volume as described above, joining the two meron components. The width of this volume joining the merons increases with increasing separation between the merons, and the maximum width at the midpoint is approximately 4, 4.5, and 6 for $d = 10, 12$, and 16 respectively. The only effect of a few cooling sweeps applied to these configurations is a small change in the positions and widths of the merons, and the resulting monopole and vortex content is the same as described above relative to the new positions of the merons.

Finally, it is interesting to consider how the monopole and vortex content we found for the meron pair connects with the two limiting cases discussed before, an isolated instanton and a single meron. If we think of an instanton as a meron pair and dissociate it into two separated merons (keeping one of them fixed at the origin), we see that the monopole content of the instanton, a point at the maximum, becomes a loop of the form shown in figure 2B joining both merons. As we continue to separate both components, this loop becomes larger, and when one of the components approaches infinity, this loop joins the meron at the origin with the meron at infinity, the result we have already discussed for the single meron solution. The same argument is valid for the vortex content. As we separate the merons, a vortex surface joins both components, and as the separation approaches infinity, in the vicinity of one meron the surface locally looks like the planar vortex surface of a single meron.

5 Conclusions

We have investigated the monopole and vortex content of a meron pair by calculating the points at which the gauge transformation fixing the gauge to the Laplacian Center Gauge is ill-defined. Threefold degeneracy of the lowest eigenvalues of the Laplacian allows the choice of different pairs of vectors to define the Laplacian Center Gauge, giving rise to different pictures for the monopole and vortex content of the configuration. The determinant of these three eigenfunctions at each lattice point defines the locus of all the points that can be monopoles or vortices. This locus is a three-dimensional volume joining both merons, and at each time plane between the merons, the locus is the surface of a sphere with its center on the line connecting the merons, and with a diameter given by the width of the curve shown in figure 2B. One particular choice of degenerate eigenvectors has a monopole line joining both merons in the xt plane for the first vector and in the yt plane for the second vector. The corresponding vortex surface looks like an ellipsoid of revolution around the t axis in the x, y, t coordinates. Many other choices of two combinations of the three degenerate eigenvectors are possible, but all monopole lines and vortex surfaces must lie in the volume where the determinant vanishes. In particular, this implies that at the position of the meron, the vortex must always be in a purely spatial plane and can never be in a space-time plane.

We have also investigated the vortex content of the meron pair by calculating Wilson loops in all Cartesian planes containing the merons. This calculation showed that as in the case of an isolated meron, each meron in a pair behaves like a source or sink for flux in non-trivial elements of the center of the group for all six planes defined by the Cartesian axes and thus corresponds to the intersection of orthogonal pairs of vortices. Thus the Wilson loops imply that in addition to a vortex at the position of a meron in a purely spatial plane, there must also be a second vortex in a space-time plane.

Although these two complementary investigations have provided interesting insight into the vortex structure of a meron pair, it is clear from comparing the results that Laplacian Center Gauge fixing is not a sufficiently powerful tool to reveal the full structure of intersecting vortices. Whereas Wilson loops clearly imply the intersection of both spatial and space-time vortices at the merons, Laplacian Center Gauge fixing only finds vortex

surfaces joining the two merons that intersect the merons in spatial planes. We note that the high symmetry of the background field produces a highly atypical situation including, for example, the intersection of monopole loops and a high degeneracy of equivalent solutions. It is possible that the introduction of a small perturbation would not only remove the intersections and degeneracy, but also produce a more generic situation of intersecting vortices. If this is not the case, more powerful techniques will be required to fully analyze the vortex structure.

Finally, looking at the combination of the results we obtain for the meron pair from Wilson loops and Laplacian Center Gauge fixing, it is reasonable to conclude that in a pair as well as in isolation, a meron is a localized source of monopole trajectories and a localized object with topological charge $\frac{1}{2}$ carrying center flux in six orthogonal space-space and space-time planes.

References

- [1] A. A. Belavin, A. M. Polyakov, A. S. Schwartz and Yu. S. Tyupkin, Phys. Lett. B59 (1975), 85.
- [2] R. C. Brower, D. Chen, J. W. Negele and E. Shuryak, Nucl. Phys. Proc. Suppl. 73 (1999), 512 [hep-lat/9809091].
- [3] V. de Alfaro, S. Fubini and G. Furlan, Phys. Lett. B65 (1976), 163.
- [4] C. G. Callan, R. Dashen and D. J. Gross, Phys. Lett. B66 (1977), 375; Phys. Rev D17 (1978), 2717; Phys. Rev. D19 (1979), 1826.
- [5] G. 't Hooft, Nucl. Phys. B153 (1979), 141.
- [6] G. 't Hooft, Commun. Math. Phys. 81 (1981), 267.
- [7] M. García Pérez, A. González-Arroyo and B. Söderberg, Phys. Lett. B235 (1990), 117; M. García Pérez and A. González-Arroyo, J. Phys. A26 (1993), 2667 [hep-lat/9206016].
- [8] A. González-Arroyo and P. Martínez, Nucl. Phys. B459 (1996), 337 [hep-lat/9507001].

- [9] G. 't Hooft, in: *High Energy Physics*, Proceedings of the EPS International Conference, Palermo 1975, A. Zichichi, ed., Editrice Compositori, Bologna 1976.
S. Mandelstan, Phys. Rep. 23 (1976), 245.
- [10] G. 't Hooft, Nucl. Phys. B190 (1981), 455.
- [11] G. 't Hooft, Nucl. Phys. B138 (1978), 1.
J. M. Cornwall, Nucl. Phys. B157 (1979), 392.
G. Mack, in: *Recent Developments in Gauge Theories*, edited by G. 't Hooft et al (Plenum, New York, 1980).
H. B. Nielsen and P. Olesen, Nucl. Phys. B160 (1979), 380.
J. Ambjorn and P. Olesen, Nucl. Phys. B170 (1980), 60; 265.
- [12] A. González-Arroyo and Á. Montero, Phys. Lett. B442 (1998), 273 [hep-th/9809037];
Á. Montero, Phys. Lett. B483 (2000), 309 [hep-lat/0004002].
- [13] M. Engelhardt and H. Reinhardt, Nucl. Phys. B567 (2000), 249 [het-th/9907139].
- [14] O. Jahn, F. Lenz, J.W. Negele and M. Thies, Nucl. Phys. Proc. Suppl. 83 (2000), 524 [hep-lat/9909062].
- [15] J. M. Cornwall and G. Tiktopoulos, Phys. Lett. B181 (1986), 353; J. M. Cornwall, Phys. Rev. D61 (2000), 085012 [hep-th/9911125].
- [16] R. C. Brower, K. Orginos and C-I Tan, Phys. Rev. D55 (1997), 6313 [hep-th/9610101].
- [17] F. Bruckmann, T. Heinzl, T. Vekua and A. Wipf, Nucl. Phys. B593 (2001), 545 [hep-th/0007119].
- [18] J. M. Cornwall, hep-th/0112230.
- [19] C. Alexandrou, M. D'Elia and P. de Forcrand, Nucl. Phys. Proc. Suppl. 83 (2000), 437 [hep-lat/9907028]; Nucl. Phys. A663 (2000), 1031 [hep-lat/9909005].
- [20] P. de Forcrand and M. Pepe, Nucl. Phys. B598 (2001), 557 [hep-lat/0008016].
- [21] H. Reinhardt and T. Tok, Phys. Lett. B505 (2001), 131.

- [22] J. V. Steele and J. W. Negele, Phys. Rev. Lett. 85 (2000), 4207 [hep-lat/0007006].
- [23] T. Kalkreuter and H. Simma, Comput. Phys. Commun. 93 (1996), 33 [hep-lat/9507023].